A Thermal Study on Small Synchronous Reluctance Machine in Automotive Cycle

M. A. H. Rasid*, A.Ospina**, K. El Kadri Benkara**, V. Lanfranchi**

*Faculty of Mechanical Engineering, Universiti Malaysia Pahang, Malaysia
** EA1006 Laboratoire Electromecanique, Université de Technologie de Compiègne, Sorbonne Universités, France

***Abstract*— Embedded automotive application has one of the harshest environment for electrical machine, especially in terms of thermal requirement. In this study, thermal evaluation of a small synchronous reluctance (Syncrel) machine intended to be used as clutch actuator is presented. A lumped parameter (LP) thermal model was built and validated experimentally. The results of the model subjected to a standardized WLTP cycle shows that the machine is thermally robust and apt for automotive application.**

Keywords*— Synchronous reluctance machine, automotive application, thermal modeling, lumped parameter model, WLTP cycle.

I. INTRODUCTION

Functions in automotive that are being electrified involve more crucial and complex applications such as clutches, power steering, assisted brakes and others. Main requirements that are common to these applications can be divided into three categories: machine performance, volume and weight, and cost (Fig. 1). For thermal aspect, it becomes particularly challenging as these applications are often placed in a particularly high temperature environment (up to 140°C in the engine compartment).

For a machine without permanent magnet, the conductor insulator is the component to be monitored carefully. Depending on the thermal class of the insulator, the critical temperature Tmax over which it will be deteriorated can be situated from 150°C to 240°C [1]. Having a precise and reliable thermal model predicting the temperature evolution in the stator slot of the machine is therefore essential in order to design an optimized machine.

II. STUDY BACKGROUND

A. Clutch actuator application

A project named e-Clutch [5] project started in 2006 had an objective of replacing actual clutch actuator system that used a DC motor along with a spring compensation system as shown in Fig. 2. We wanted to have a less encumbering system (exterior diameter less than 43.5mm), with a more reliable motor that can be directly integrated into the housing of the clutch system. The condition in the clutch housing includes

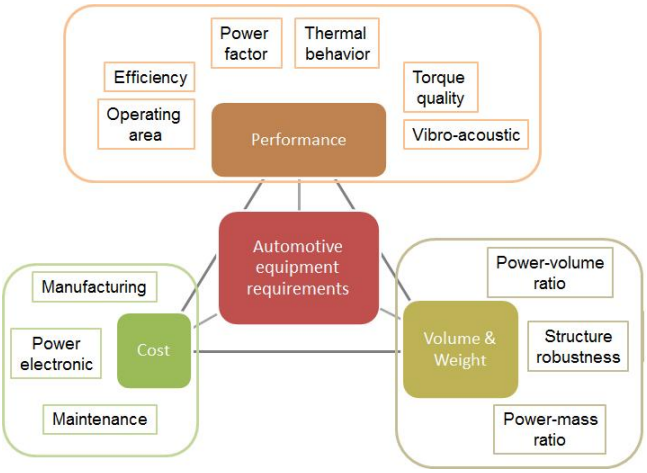

Fig. 1. Requirements related to automotive equipment actuator.

high ambient temperature (140°C), tight space and intrusion of dust, oil and eventual used clutch lining.

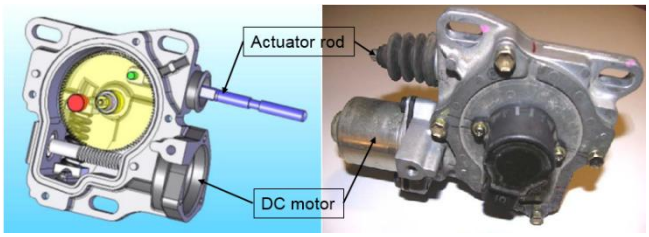

Fig. 2. The clutch actuator by compensation system, which can be found for example in the Toyota Aygo MMT. The whole system is then mounted onto the transmission system housing.

B. Syncrel with segmented rotor

Recent studies have shown that the Syncrel motor can be suitable for this type of application [2, 3, 4]. Taking into account requirements mentioned above along with manufacturing cost and feasibility, a totally enclosed non-ventilated Syncrel motor with segmented rotor was designed and prototypes were built. It is a 2 pole pair motor with passive segmented rotor and distributed winding. The

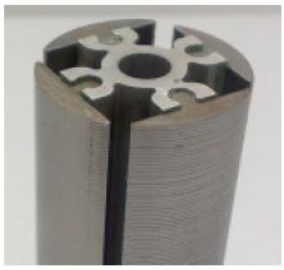

(a) Complete mounted rotor

(b) Mounting the teeth on the bearing housing

(c) Complete winding on the already mounted teeth.

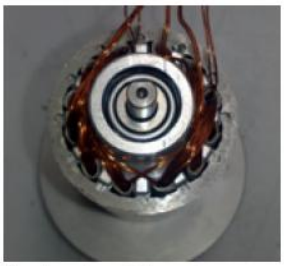

(d) Completed Syncrel motor assembly.

Fig. 3. The assembly of the Syncrel machine prototype.

conductor used is a class H that can withstand up to 220°C. Parts of the motor during its mounting can be seen in Fig. 3.

III. Thermal Model

A. LP model

Lumped parameter modeling has been chosen thanks to its best compromise between computation cost and reasonable accuracy, provided that the network is chosen carefully. The construction of an LP model can be divided into three steps:

- Identification of heat transfer mechanism.
- Definition of thermal parameters of each part of the machine.
- Validation of the model and eventual fitting.

1) Heat transfer

The three main mechanisms of heat transfer in a motor are conduction (1), convection (2) and radiation (3). The heat transfer rate of each mechanism can be written as below [6].

$$\dot{Q}_{cond} = \frac{dQ_{cond}}{dt} = -\lambda A \frac{dT}{dx} \quad (1)$$

$$\dot{Q}_{conv} = \frac{dQ_{conv}}{dt} = -hA.\Delta T(t) \quad (2)$$

$$\dot{Q}_{rad} = \sigma.A.\varepsilon.F_{1-2}\left(T_1^4 - T_2^4\right) \quad (3)$$

The three heat transfer mechanisms occur in our motor. Several hypothesis can however be made: Conduction occurs across every solid parts while convection and radiation occur in the air gap, interior cavity and on the exterior surface in contact with ambient air. Convection in a small air gap and cavity can be considered negligible compared to conduction as the Nusselt number which represents the ratio of convective to conductive heat transfer across the surface is very small [7]. Radiation in air gap and cavity can also be considered internally negligible especially for a compact motor and it can be explained by a low temperature gradient. For convection and radiation on exterior surface of the motor, both are going to be integrated into a single thermal resistance R_{ext} found by experimental identification.

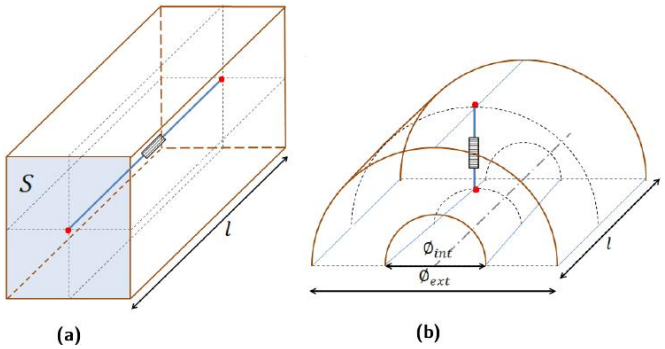

Fig. 4. Thermal resistance representation in extruded surface (a) and cylindrical (b) generic form for a 1D heat transfer.

2) Thermal parameters calculation

a) Thermal resistance

For conduction, there are several generic simple form on which the thermal resistance can be calculated easily: extruded profile form, cylindrical shells and spherical shells.

Considering our application, only extruded profile and cylindrical shells are going to be used. In a one direction heat transfer, Fig. 4a illustrates the integration of a thermal resistance representing conduction heat transfer across an extruded profile form of a section *S*. The thermal resistance $R_{cond\ extr}$ (W/m².K) can be calculated as in equation (4).

$$R_{cond\ extr} = \frac{1}{\lambda}\frac{l}{S} \quad (4)$$

Fig. 4b illustrates the integration of a thermal resistance representing conduction heat transfer across a cylinder section with the interior diameter of $\emptyset_{int}$ and the exterior diameter of $\emptyset_{ext}$. The conduction thermal resistance of cylindrical shell $R_{cond\ cyl}$ (W/m².K) can be calculated as in equation (5).

$$R_{cond\ cyl} = \frac{1}{\alpha l}\ln\left(\frac{\emptyset_{ext}}{\emptyset_{int}}\right) \quad (5)$$

However, application on electrical machine means that the heat transfer need to be modelized in three directions: radial, axial and ortho-radial. It is important to define the connection point and ensure that the right temperature can be deduced from the model. Fig. 5 shows a simple cuboid element as example with all radial, axial and ortho-radial resistances being sectioned into half. Their thermal resistance (R_{rad}, R_{ax} and R_{ortho}) are calculated regarding their respective perpendicular surfaces (S_{rad}, S_{ax} and S_{ortho}) and the distances to the extremities of the surfaces using equation (4). The middle point between the thermal resistances of each direction are connected together, giving access to the average

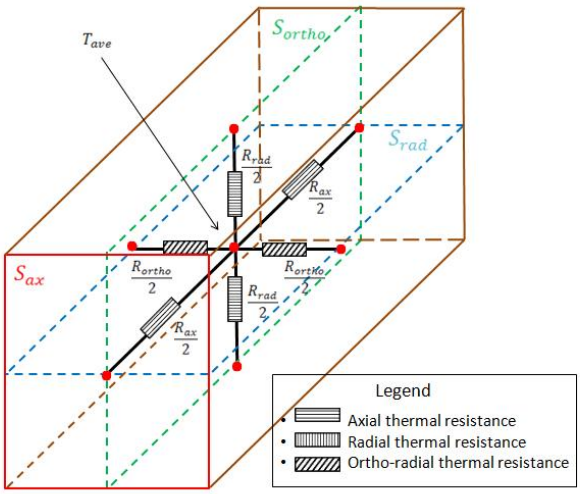

Fig. 5. Connection between radial, axial and ortho-radial thermal resistance and the average temperature deduced from the model configuration.

temperature of the cuboid body, T_{avg}. The other points on the extremities of each direction give the surface temperature in the direction. They are also the points that are going to be connected with neighboring bodies.

b) Thermal capacitance

In order to be able to evaluate the transient state, thermal capacity of each body C_{th} (J/K) are also integrated into the model. They are calculated using their material's specific heat capacity c (J/kg.K), density of (kg/m^3) and volume V (m^3) (Equation (6)).

$$C_{th} = \rho . V . c \tag{6}$$

In the lump body such in Fig. 4, the capacity of the body will be connected to the center point, at the same point where T_{avg} can be found.

3) Application on Syncrel prototype motor

The machine is discretized in function of generic forms having a homogenous material characteristics. From a cross-sectional view in Fig. 6, we can classify 7 elementary parts which are: casing, stator yoke, teeth, slot set, air gap, the rotor assembly and shaft. The radial and ortho-radial supposed heat flux presented by red arrows while the axial heat flux are in the direction perpendicular to the surface represented.

Fig. 7 shows that there are three other parts to be taken into account in the axial heat transfer direction: end-winding, air cavity and flange-bearing set.

The rotor structure which is composed of ferromagnetic active segments, aluminum holder and air was homogenized into a single rotor assembly. Its homogenized structure thermal resistance was calculated by taking into account each element ratio in the assembly. This can be done because there are no major losses to be injected on a specific point and the losses in the ferromagnetic segment are also negligible.

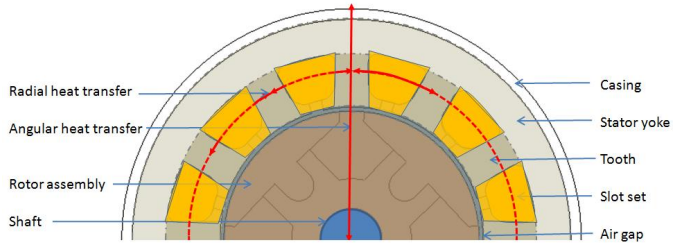

Fig. 6. Elementary parts in simplified geometry form with the supposed heat flux. In each elementary part, a resistance representing the elements thermal resistance is calculated (Table I).

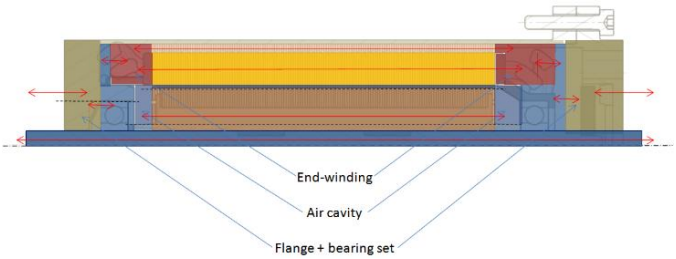

Fig. 7. Axial heat transfer including the end-winding, air cavity and the flange and ball bearing set as elementary parts. In each elementary part, a resistance representing the elements thermal resistance is calculated (Table I).

With a passive rotor, there are also no critical elements in the rotor on which the temperature need to be looked into.

The thermal resistance of equivalent material of the slot is computed using homogenization method [8]. The alteration of thermal resistance in ferromagnetic parts due to stacking is also taken into account by integrating the stacking factor and the adhesive resin properties that was used in the sheet stack [9]. A surface contact thermal resistance is also taken into account at the largest surface contact (stator yoke-casing by using an equivalent effective air gap thickness in its computation [10].

The resulting complete LP model is shown in Fig. 8.

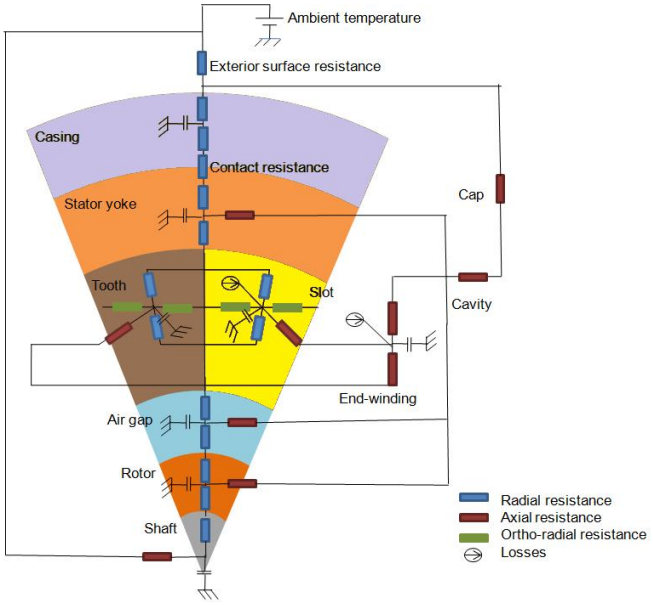

Fig. 8. The complete LP model of the Syncrel motor.

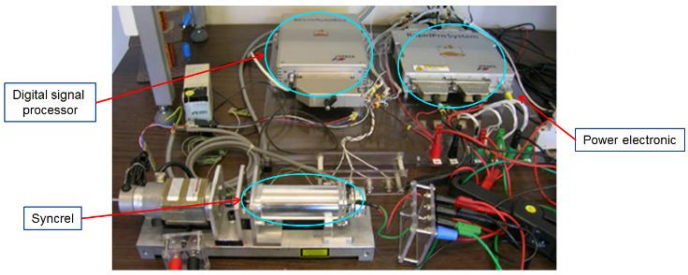

Fig. 9. The Syncrel prototype test bench.

B. Experiments

Using the prototype machine, different experiments and results will be presented in this section in regard to LP model validation. The prototype motor is mounted on a test bench (Fig. 9).

A K-junction thermocouple was inserted in one of the slot. The bench is controlled by a Dspace Micro-Autobox with command made in Simulink®. It is integrated with a Rapid-Pro power unit module for the power electronic. All the parameters managed by Micro-Autobox are observable from a PC and can be recorded for post-treatment.

1) Identification of external surface thermal resistance R_{ext}

The only thermal parameters left to be determined in our model is R_{ext}. Besides being difficult to calculate, it is important to remind that in a TENV, the most important surface on which the heat will be evacuated is the exterior surface. Thus, any error on its value will cause a big error in the slot temperature prediction. It is therefore need to be determined using experimental identification.

Theoretically, when the machine has a stable temperature (steady state), it is supposed that the heat input (generated internally) is equal to the heat output (evacuated by convection and radiation through the outer surface of the machine). The temperature on the surface can also be considered homogenous as the outer surface is constituted by a metallic casing with a very high thermal conductivity. Therefore a one node model can be applied over the entire surface and can be modelized by equation 1.

$$T_{surf}(t) - T_{amb}(t) = Q_{th} \cdot R_{ext}\left(1 - e^{-t/\tau}\right) \qquad (2)$$

with $= R_{ext} \cdot C_{total}$; C_{total} is the thermal capacity of the machine and its test bed.

As it attains steady state ($t \to \infty$), the temperature difference between the machine surface and the ambient air at steady state is the product of machine exterior thermal resistance R_{ext} (convection and radiation) and the heat input Q_{th}. It is important to note that for R_{ext} identification, the first degree equation is properly used here as the interface between the exterior surface and ambient air is only one node.

Practically, copper losses was generated by means of injecting direct current into the winding and the machine is left heating until it reaches the steady state. The temperature on the surface of the machine is registered via a thermocouple installed on its surface while the ambient temperature is the same thermocouple reading before the experiment started (t = 0). Knowing the winding resistance and the current injected, thus the copper losses generated Q_{th}, R_{ext} is then deduced. To ensure the robustness of the method in obtaining R_{ext}, the experiments is done on three current level and R_{ext} was found to be around 1.6 and 1.7 for our test bench set-up (Table I). $R_{ext} = 1.6$ is used in the LP model.

TABLE I
DEDUCTION OF R_{EXT} USING EXPERIMENTAL IDENTIFICATION AT STEADY STATE.

Losses, $\dot{Q}_{th}$ (W)	T_{surf} (°C) Steady state	T_{amb} (°C)	R_{ext}
1.3	25.5	23.0	1.7
5.2	32.5	24.0	1.6
10.9	42.0	25.0	1.6

2) Validation of the complete LP model

In order to validate the model in both transient and steady state, both total thermal resistance and total thermal capacity need to be verified and validated. Therefore this validation step comprises two separate validation: the total thermal capacity validation and the complete model validation in copper losses configuration.

a) Verification of the total thermal capacity of the machine

The total thermal capacity C_{total} of the motor and its test bed has been verified using an experimental identification and fitting method. This was done by fitting the curve of temperature rise on the surface T_{surf} of the machine to a first degree equation (equation (1)) so as to identify C_{total} of the machine set. Like in *B.1*, this method considering one node is also valid as the identified capacity is C_{total}, which is the sum of capacity of all the motor components. The identified C_{total} has been compared to the calculated capacities and it shows good agreement with C_{total} equal to approximately 500 J/K.

b) Validation of the complete model in copper losses configuration

Losses in a motor originate from different sources: copper losses, magnetic losses and mechanical losses among others. Apart from copper losses, estimation of other losses are difficult, thus can introduces uncertainties in model validation process. By having a copper losses experimentation, losses estimation uncertainties can be reduced. As mentioned in Introduction, the most important part to be observed is the winding, thus the validation is done on the slot temperature and it will be compared to the LP model simulation in similar condition.

To do so, an experiment set-up where losses generated form direct current step was injected into the three phase of the stator winding. The temperature rise is registered until the steady state is attained. To ensure the robustness of the model, the test was done on three different operating points. The comparisons are shown in Fig. 10. The precision of the K-junction thermocouple used is at ±1°C and the current

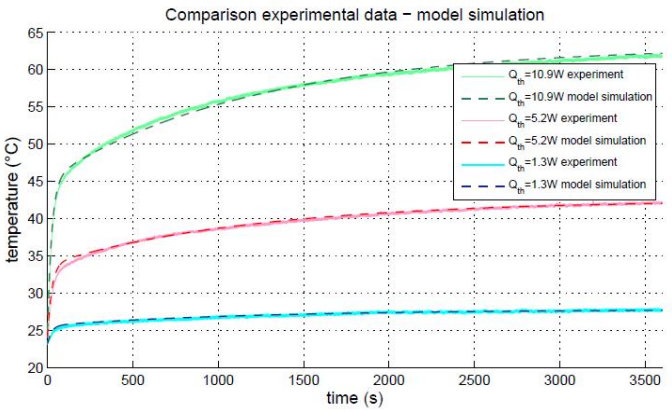

Fig. 10. Model simulation and experimental winding temperature comparison on different losses injected.

measurement by the shunt is at ±0.25%. It was concluded then that the LP model is precise and robust for copper losses configuration.

IV. Simulation under Clutch Duty Cycle

It is in the upmost interest to test the machine using a realistic cycles which represent the motor intended utilization. In case of an automobile clutch, simulations can be done using a cycle representing the actual clutch actuating operation deduced form a standardized automotive driving cycle. In our case, we use the latest global standard that has been finalized by United Nation Economic Commission for Europe (UNECE), called WLTP cycles [11]. The WLTP procedure includes three test cycles applicable to vehicle categories of different power-to-mass ratio that go through different speed phases.

The prototype machine is intended to be used as a clutch actuator thus, the machine can be used for all 3 class of automobile cycles. All of them will be then simulated. To begin, certain information linked to the clutch actuation need to be extracted from the cycles above.

There are 3 main information needed to make the simulation:

1. The operating period of the machine to actuate the clutch in order to make gear change.
2. The current intensity fed into the machine in order to actuate the clutch.
3. The moment when the clutch is actually actuated.

For the operating period of the clutch actuator, Doc [5] has mentioned that the final design of the machine allows it to deliver torque profile as shown in Fig. 11. From the torque profile, the period and the current intensity to operate the machine were deduced. It can be seen that the torque profile are non-linear. In order to simplify the heating simulation, a simplified linear torque profile set at the maximum torque value will be used as input in order to make sure that the simulated heat rise is not underestimated. The most critical case that will push the temperature of the winding to the highest point is the non-assisted mode with maximum torque. This gave us the linear operating torque in Fig. 12.

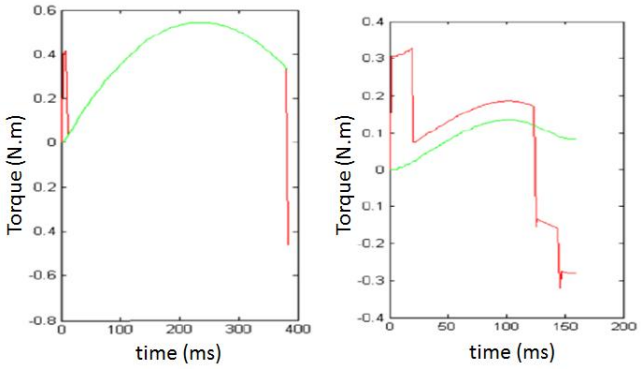

Fig. 11. The Syncrel machine torque profile in non-assisted (left) and assisted (right) mode in function of time for clutch engagement [5].

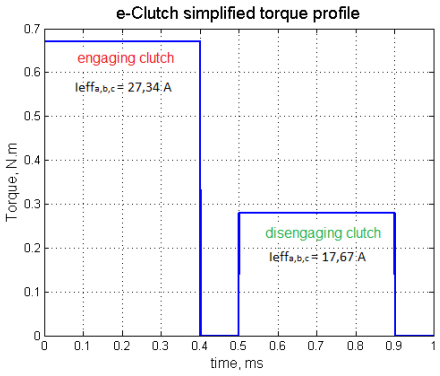

Fig. 12. The simplified linear torque profile with the deduced current.

For Syncrel machine operating moment, it can be easily extracted from the cycle. Each car has an optimal speed for each gear change. Table II (a) provides a general guide for the speed on which the gear would be changed up or down. The number of gear changes in each cycle is shown in Table II (b).

TABLE II
GEAR CHANGES IN EACH WLTP CYCLE

(a)

Speed (km/h)	Gear change
0	First
10	Second
30	Third
50	Fourth
70	Fifth

(b)

Cycle	Number of gear changes
C1	37
C2	92
C3	99

The speed profiles and the moment the Syncrel motor actuates the clutch in all three WLTP cycles are shown next in Fig. 13.

The machine heating resulting from the clutch actuation in different WLTP cycles in an ambient temperature of 25°C are shown in Fig. 14. It can be seen that, as the gear changes rapidly at the moment of acceleration or deceleration, the winding temperature rise instantaneously as the heat does not have time to be evacuated, thus a higher temperature peak can be observed. This can be especially observed in the cycle where the vehicle is able to accelerate and speed up to the fifth gear (WLTP C2 and C3). Whereas for WLTP C1, the low speed profile limit the sequential gear changes. The maximum

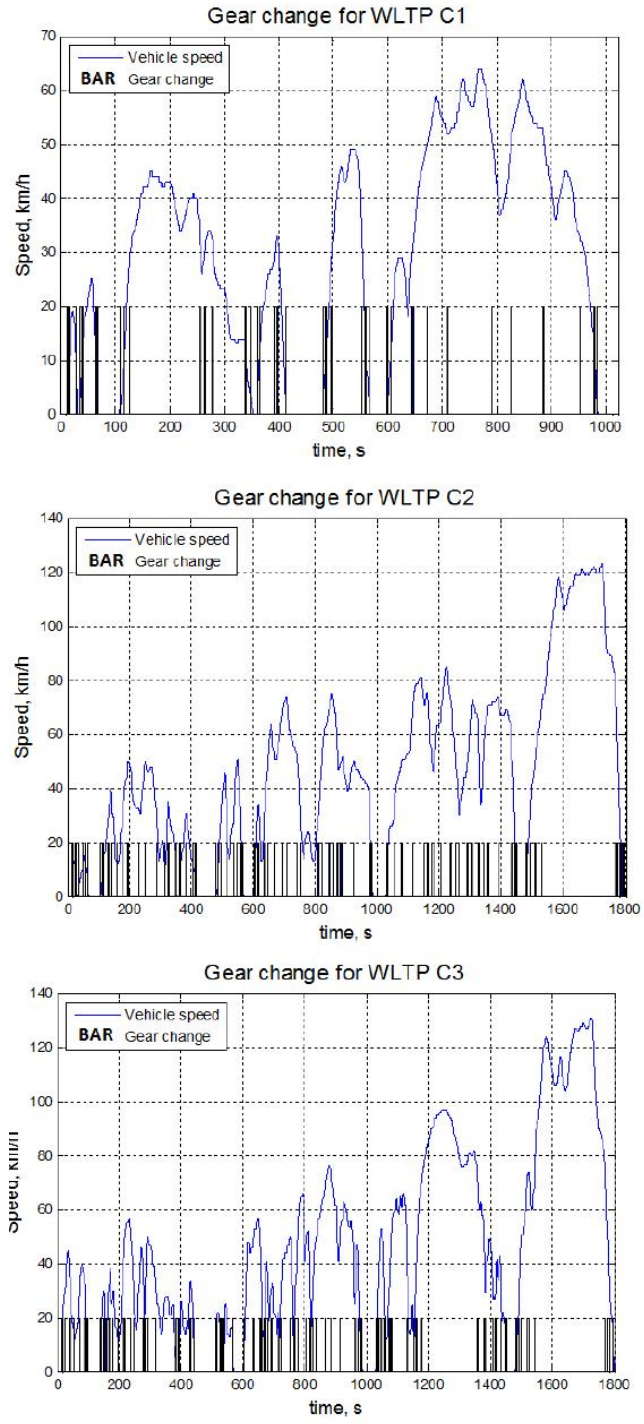

Fig. 13. The vehicle speed and the gear changes for all three WLTP cycles.

temperature rise observed is in C3 with $\Delta T = 45°C$.

In an ambient temperature of the clutch environment at 140 °C (as stated in II.A), the winding temperature rise found for C3 cycle can be seen in Fig. 15. The maximum temperature reaches 198°C and ΔT is higher than 45°C. This is due to higher thermal resistance of the winding affected by the high ambient temperature. The maximum temperature is nonetheless lower than the rated temperature of the conductor (220°C), thus the machine can survive in the clutch housing.

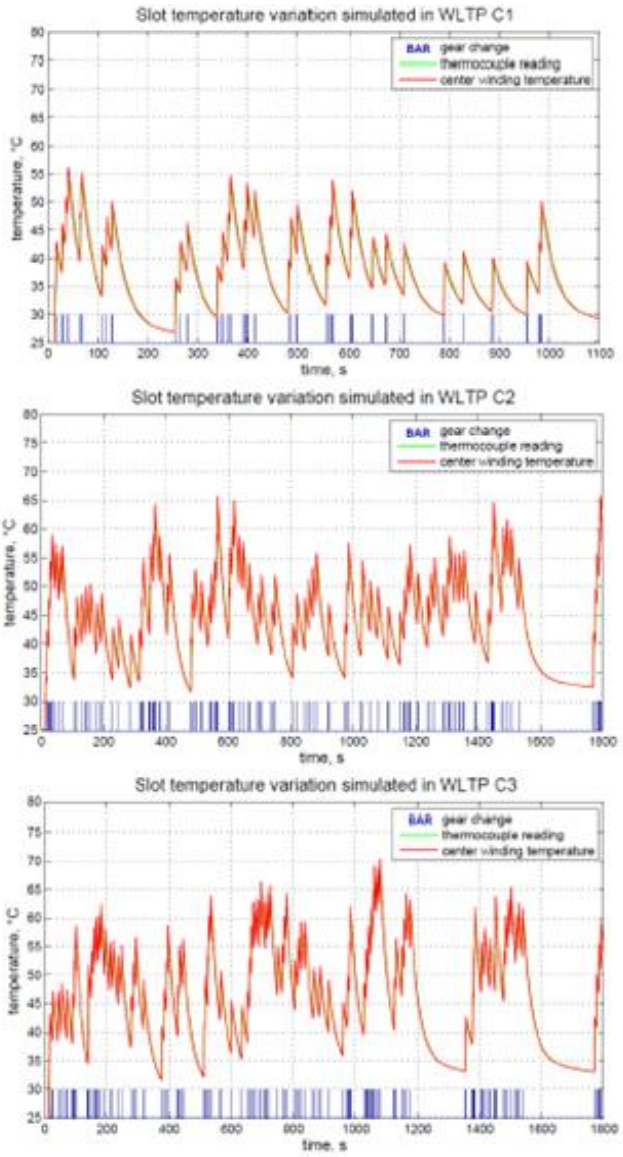

Fig. 14. The temperature rise in the winding of the Syncrel motor due to clutch operation for all three WLTP driving cycles.

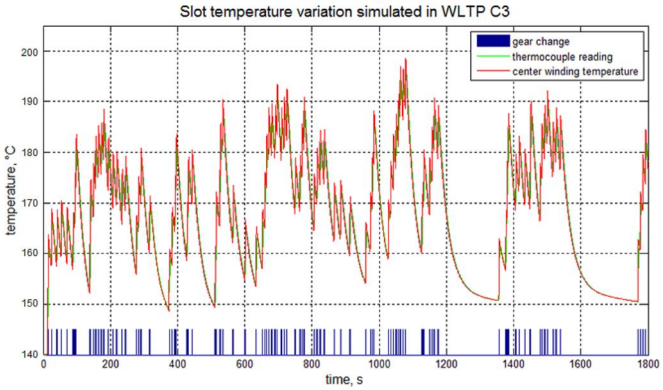

Fig. 15. The temperature rise in the winding of the Syncrel motor due to clutch operation for all three WLTP driving cycles.

V. CONCLUSION

The thermal behavior of a segmented rotor Syncrel machine in an electric clutch application was studied in this paper. An LP thermal model was built and shown to be precise and robust in experimental validation. Following the validation, the model was used to simulate the temperature rise of the winding in WLTP cycles. Results show that the Syncrel with segmented rotor machine is thermally capable and suitable for this particular application. This could also be the case for other similar applications.

REFERENCES

[1] H. Rosen, R. Mayschak. UL1446-A practical Electrical Insulation Standard. Electrical Insulation Magazine, IEEE. Sept. 1985.

[2] Moghaddam, R.R.; Magnussen, F.; Sadarangani, C., "Theoretical and Experimental Reevaluation of Synchronous Reluctance Machine," Industrial Electronics, IEEE Transactions on , vol.57, no.1, pp.6,13, Jan. 2010

[3] Boldea, I.; Tutelea, L.; Parsa, L.; Dorrell, D., "Automotive Electric Propulsion Systems with Reduced or No Permanent Magnets: an Overview," Industrial Electronics, IEEE Transactions on , vol.PP, no.99, pp.1,1

[4] Boglietti, A.; Cavagnino, A.; Pastorelli, M.; Staton, D.; Vagati, A., "Thermal analysis of induction and synchronous reluctance motors," Industry Applications, IEEE Transactions on , vol.42, no.3, pp.675,680, May-June 2006

[5] Doc C., "Contribution à la Conception et au Dimensionnement d'un Actionneur d'Embrayage". Ph.D. Thesis, Université de Technologie de Compiègne. 2010.

[6] Holman, J.P., Heat Transfer, McGraw-Hill, New York, 1997.

[7] Bouafia M.; Bertin Y.; SaulnierJ.B.; Robert P., " Experimental analysis of heat transfer in a narrow and grooved annular gap with rotating inner cylinder ", International Journal of Heat and Mass Transfer, 41, n° 10, p. 1279-91, 1998.

[8] T. Mori, K. Tanaka, "Average stress in matrix and average elastic energy of materials with misfitting inclusions", Pro. R. Soc. Lond A 417, pp. 59-80, 1988.

[9] B. Renard, "Etude expérimentale et modélisation du comportement thermique d'une machine électrique multi-fonctions. Applications à un alterno-démarreur intégré", Ph.D. dissertation, Université de Poitiers, 2003.

[10] Staton, D.; Boglietti, A.; Cavagnino, A., "Solving the More Difficult Aspects of Electric Motor Thermal Analysis in Small and Medium Size Industrial Induction Motors," Energy Conversion, IEEE Transactions on , vol.20, no.3, pp.620,628, Sept. 2005

[11] Tutuianu M., Marotta A., Steven H., Aricsson E., Haniu T., Ichikawa N., Ishii H., "Development of a World-wide Worldwide Harmonized Light Duty Driving Test Cycle (WLTP)," technical report, 68th GRPE, 7-10 January 201 4.